An iron production and exchange system at the center of the Western Han Empire: Scientific study of iron products and manufacturing remains from the Taicheng site complex

Wengcheong Lam[a,*], Jianli Chen[b], Jianrong Chong[c], Xingshan Lei[b], Wai Lun Tam[d]

[a] Department of Anthropology/History, The Chinese University of Hong Kong, Hong Kong, China
[b] School of Archaeology and Museology, Peking University, China
[c] Shaanxi Provincial Institute of Archaeology, China
[d] Institute of Archaeology, UCL, UK

ARTICLE INFO

ABSTRACT

The discovery of a small-scale ironworks and ironware from burials at the Taicheng site complex in the Wei River Valley, Shaanxi, provides a valuable chance to systematically examine not only manufacturing technology but also the distribution system of iron objects within the region surrounding the Western Han Empire's capital city. According to metallurgical and SEM-EDS analyses, the ironworks primarily employed melting/casting techniques to manufacture agricultural tools via recycled scrap iron and imported iron semi-products from other manufacturing centers. In addition, forging and, possibly fined iron manufacturing, were identified through the discovery of hammer scale and slag. The artefactual evidence from a nearby cemetery shows that solid-state decarburization of cast iron and fined iron were employed intensively in the manufacturing of iron tools buried as grave goods, but these were unlikely to be manufactured entirely and directly by the local ironworks. By integrating other lines of evidence (e.g., ceramic casting molds), we suggest that, since local, small ironworks like Taicheng only focused on agricultural tools, the supply of most daily iron objects was met via commodity exchange. The study proposes that the local iron industry employed a strategy of "diversification" in order to maximize both the sources of raw materials and supply of final objects, and the exchange or transportation of ironware played an essential role in the development of the iron industry during the Han period.

1. Introduction

The cast iron (i.e., iron that was melted and cast, usually with about 4% of carbon; see Wagner, 1993:336) industry in ancient China was unmatched in the preindustrial world in terms of its scale and development. From the 7th to 5th century BCE, cast iron technology was gradually established in the Central Plains as well as in different peripheral states (Lam, 2014). By the dawn of the Qin unification (221 BCE), the rapid increase in the use of iron resulted in the development of both solid-state decarburization of cast iron and malleable cast iron (Han and Chen, 2013; Han and Duan, 2009). Iron gradually replaced other major types of tool manufacturing materials and became an essential commodity in the financial system of the Han Empire (206 BCE-202 CE), especially when iron mining and production came under the Empire's direct control after the implementation of the well-known "iron and salt monopoly" in 117 BCE (Wagner, 2008:192–210, 246).

In previous decades, discoveries of large ironworks sites such as

Guxing (Zhongguo, 1978), Wafengzhuang (Li, 1995), Wangchenggang (Chen et al., 2011; Henan and Lushan, 2002), and Linzi (Du et al., 2011; Du et al., 2012), provided important evidence for addressing the technology of the Han iron industry as a whole. However, these cases are all adjacent to rich iron resources, while the iron industry in places without sufficient iron deposits was not represented in the literature. Therefore, addressing the question of production in areas without rich iron resources became crucial to developing an understanding of the basic economic infrastructure whereby ironworks of various scales were integrated into the imperial system.

This article presents the analytical results of iron manufacturing waste from an iron workshop at a site called Taicheng in the Wei River Valley, Shaanxi (Fig. 1), and iron objects used as burial goods from a cemetery in the same community. Even though the Wei River Valley was recognized as the political core of the Western Han, its iron industry was still underexplored because only a handful of artifacts, mostly from cemeteries, had been analyzed (Beijing, 1996; Du and Han,
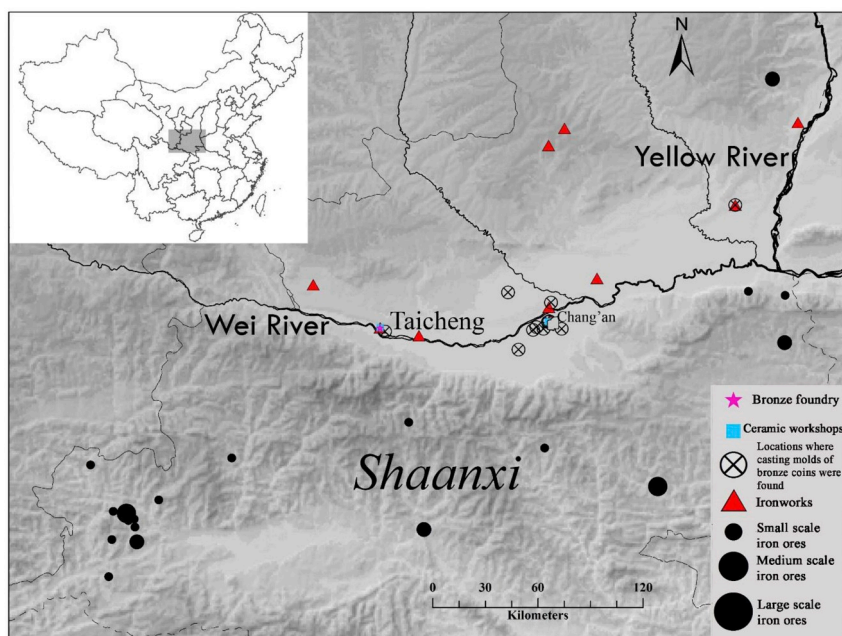
Fig. 1. Map of production remains and iron ores within the Wei River Valley and present-day Shaanxi Province. (Redrawn from Bai, 2005, Appendix 1, Shaanxisheng, 1993:152–153).

2005; Guo et al., 2014; Liu, 1999). A few ironworks have been discovered (e.g., Zhongguo, 1995; Zhongguo, 1997), but no systematic analysis has yet been conducted on manufacturing remains. This study attempts to shed light on small-scale ironworks by synthesizing the results of research into manufacturing waste from the Taicheng production site and ironware from nearby funeral contexts, with data gathered using optical microscope and scanning electron microscope (SEM) with energy dispersive spectrometry (EDS) in order to reconstruct the iron industry in the Taicheng settlement.

2. Case study: the iron foundry and Han cemetery in the Taicheng site complex

The Taicheng foundry, located in Yangling city, Shaanxi province, about 70 km west of present-day Xi'an (Fig. 1), was the first well-investigated site of its type in the region of the Wei River Valley. Based on archaeological reconnaissance and excavation conducted in 2011, Taicheng was identified as a small-scale ironworks covering an area less than 10,000 m² (Fig. 2) and roughly dated to the Early Western Han period (~202-140 BCE) (Zhao et al., 2012). In this article, the term "small-scale" is determined based on a comparison with other well-excavated large ironworks (e.g., Wafangzhuang covering at least 28,000 m², see Li, 1995). Although only about 500 m² were excavated by our fieldworks (Shaanxi, 2018), the excavation area selected and concentrated on the part of ironworks with dense remains, based on the survey and augering results. Midden and trash pits discovered were probably the most representative features of workers' production activities that could be found from the ironworks. The excavated features contained ceramic molds and other types of debris including iron slag, iron fragments, tuyères and furnace fragments. No iron ores or furnace features have yet been discovered at the site. To the north of the ironworks in the same site complex, a large-scale cemetery in contemporary use was identified. A total of 294 tombs were excavated, providing information about the community associated with the Taicheng ironworks, but no contemporary residential components were found through survey (Fig. 2).

Therefore, iron objects from the cemetery and manufacturing debris

from the workshop collectively offered a special opportunity to achieve a better knowledge of the Han iron industry. Previous studies (Kageyama, 1984; Wagner, 2008:156–159, 186–188; Yamada, 1998) suggested that, before the implementation of the monopoly in 117 BCE, most production took the form of either small-scale household units, large-scale factory-like units controlled by the state in urban centers, and plantation-like large production sites in ore-mining areas. Because of its location situating in an area remote from iron ore deposits (Fig. 1), its small scale, and its primary operational period that was preceding the introduction of the iron monopoly, excavated remains at Taicheng ironworks might conventionally be classified as "household" production units run by family members. However, no previous study has attempted to synthesize the technological study of ironworks production of this kind with consumption data from nearby settlements, in order to address not only manufacturing techniques on a small, local scale, but also the distribution of raw materials and final products within a wider region. Based on preliminary analyses, the assemblage of ceramic molds includes two major types, hoe-head implements and plowshares (Table 1). Nonetheless, there is no evidence to suggest that any iron vessels or other types of products (e.g., iron rods for smithing) were cast at the site. This raised two important questions to be addressed by the research. Firstly, given the difficulty to transporting heavy, bulky iron ingots, did the ironworks use collected scrap iron as its only raw materials source? Also, was it possible to determine whether most objects used locally could be manufactured by the nearby ironworks? These questions can only be addressed through the study of a small-scale iron industry.

Although it is almost impossible to geochemically provenience cast iron objects due to the much-reduced levels of gangue still present, metallurgical analyses can nevertheless provide the technological profile to show, as indirect evidence at least, if the techniques used in products were similar at the production and consumption loci. This latter study was conducted by integrating three evidential components: the analysis of slag (manufacturing waste), analysis of iron fragments (potential raw materials, final products, and manufacturing waste), and analysis of iron objects from the cemetery (final products). Through the comparison of manufacturing techniques, this study attempts to
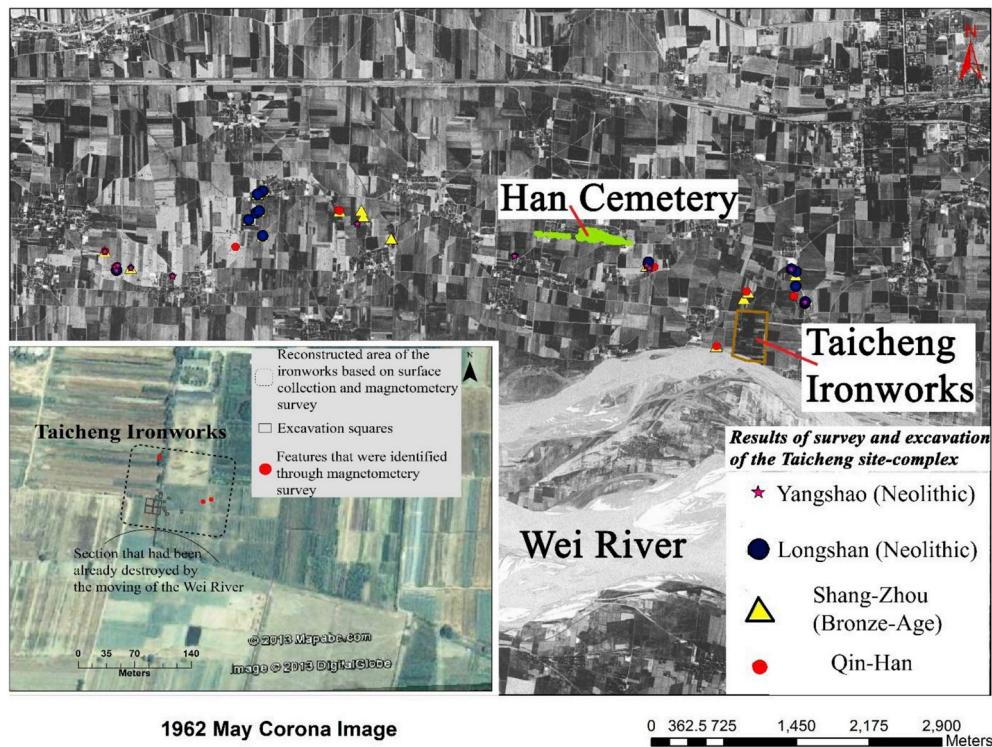
Fig. 2. Map of the Han cemetery, ironworks, and settlements of various periods identified through survey in the Taicheng site complex. Survey results did not show large-scale residential sites in contemporary with the ironworks.

Table 1
Numbers of casting molds identified at the ironworks.

	Pieces	MNI
Hoe-head implements	1139	277
Plowshares	175	58
Core in the set of casting molds of plowshares	598	162
Chisel	53	8

Note: MNI (Minimum number of individuals) refers to the fewest possible number of entire pieces of molds.

conduct a fine-grained analysis that might shed light on the operation of a small-scale ironworks in its local area and the procurement system of iron objects across the region.

3. Identification criteria and sampling process

This study employed metallurgical analyses to study representative slag (Fig. 3, Fig. 4) and iron samples from the production site (Fig. 5) and iron objects from a nearby cemetery (Fig. 6). A total of 68 pieces of slag and 130 iron objects (107 iron fragments from the ironworks, and 23 iron objects from the cemetery) were studied in this project. Slag remains and iron fragments were collected based on a preliminary classification and visual examination of all excavation samples. During the analytical process, slag remains were classified into three major categories: glassy and vitrified slag, a mixture of slag, iron and charcoal fragments (Fig. 3), and special slag (Fig. 4). Samples were selected from each of these groups. Based on their overall appearance and surface attachments, such as charcoal and slag, the iron fragments (Fig. 5) were placed into one of two major categories: potential iron tools and unidentifiable iron objects. These items could be scrap iron (raw materials for re-melting) as well as waste products, also known as bear iron, which is molten iron that has frozen in the bottom part of the furnace because of imperfect operation (Wagner, 2008:323). No complete final products were identified throughout the entire excavation.

The cemetery is in the northwest corner of the Taicheng site complex (Fig. 2). A total of 294 middle/low-rank burials have been excavated, and more than two-thirds of them date to the early Western Han period contemporary with the ironworks. A total of 77 pieces of iron were found, among which almost 50% were iron vessels (including 23 pieces of caldrons and 16 pieces of plate-shaped lamps). For the purpose of comparison, 23 iron samples covering major types of tools in the assemblage were collected, including eight ring-pommeled knives, four large knives, four swords, four small knives, one nail, one tube (attached to a halberd), one axe, one *cha* spade, and one halberd (Fig. 6).

All collected samples were prepared using a standardized procedure for metallurgical analysis. For special and important items such as fined iron objects with slag inclusion, the study employed SEM-EDS in the Department of Physics at the Chinese University of Hong Kong for chemical composition analysis. For slag inclusions (SIs) in iron objects, we employed point-scanning to collect the chemical compositions of particular features and area-scanning to collect the average chemical compositions of each SI with the voltage of 15 kv and 40-s collection time. For artifacts with no clear evidence of welding, we try to collect at least 20 SIs covering the cross-section if the sample condition is good enough. For artifacts that were made by welding, we analyzed at least 10 SIs in each welded layer with good condition. For slag samples (manufacturing waste), we collected area-scanning data from at least three spots larger than 100 μm*100 μm in order to calculate the average composition.

A complete *chaîne opératoire* of steel-making in ancient Chinese ironworks might include the steps illustrated in Fig. 7. The previous literature already identified that there were at least three ways through which wrought iron (iron with carbon content in the range 0.1–0.3%) and steel (iron with carbon content in the range 0.5–1%) were manufactured during the Warring States and Western Han period: direct reduction by using the bloomery process, fining of cast iron from a blast furnace (or fined iron below), and solid-state decarburization of cast iron from a blast furnace (Chen and Han, 2000, 2007; Wagner,

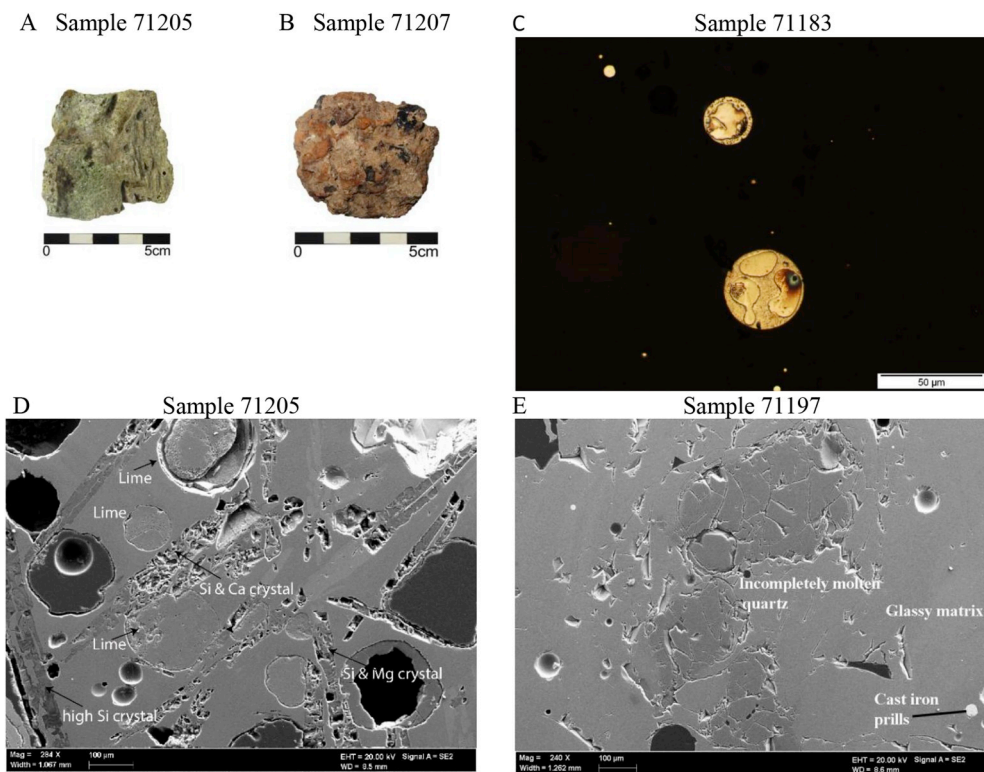A   Sample 71205   B   Sample 71207   C   Sample 71183

Fig. 3. Photos, optical photomicrographs, and SEM images of glassy slag and a mixture of slag, iron and charcoal fragments. A) top view of 71205, a typical glassy and vitrified slag. B) top view of 71207, a mixture of slag, iron and charcoal fragments. C) shows a typical microstructure of glassy slag including cast iron prills with P–Fe eutectic structure. D) is a SEM image of 71205 showing unmelted limestone and high Si crystal. E) is a SEM image of 71197 showing unmelted quartz.

1993:288). By definition, solid-state decarburization of cast iron involves the annealing of a cast iron object in an oxidizing atmosphere in order to produce wrought iron or steel for smithing (Wagner, 1993:291). In general, this process is similar to the making of malleable cast iron, i.e., annealing a white cast iron at a high temperature for a period of days to decarburize or graphitize the casting (Wagner, 1993:338, 351). The major difference is that the latter (malleable cast iron) was usually being cast in its intended final form (Wagner, 1993:291). Fined iron, also known as *chaogang* (炒钢) in Chinese literature, refers to the operation of converting cast into malleable iron in a hearth or open fire, facilitated by a blast of air with charcoal as the fuel (Percy, 1864:579; malleable iron here refers to wrought iron or medium-carbon steel, see explanation in Wagner, 1993:290–291). This finery process is also known as the "indirect process" of steel making

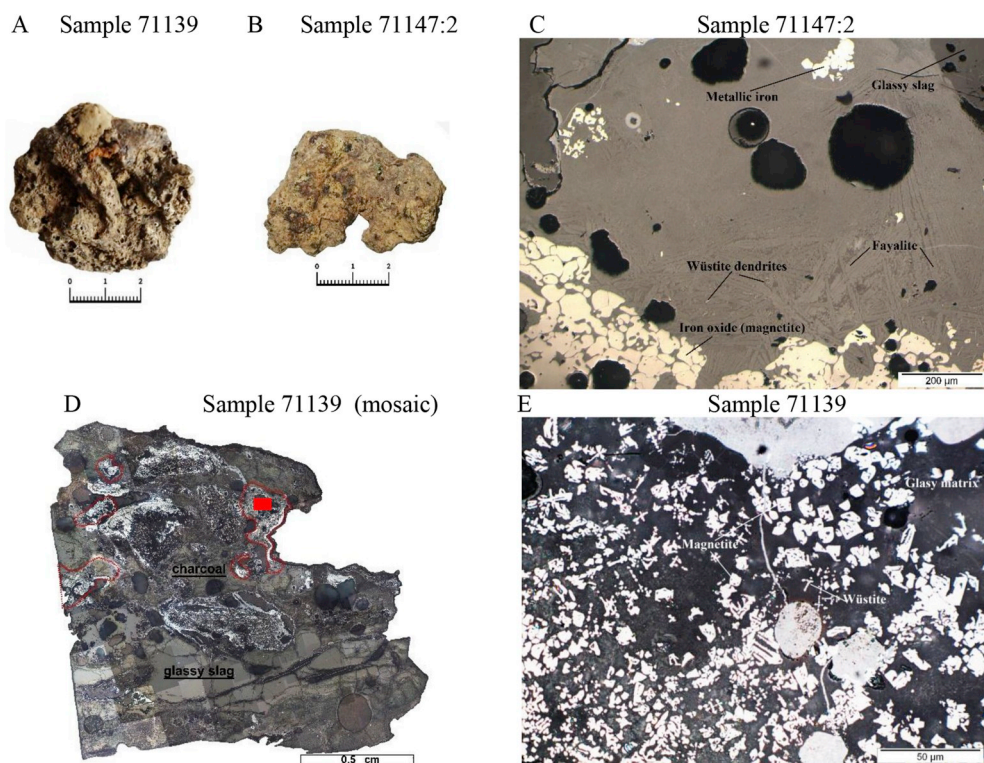A   Sample 71139   B   Sample 71147:2   C   Sample 71147:2

Fig. 4. Photos and optical photomicrographs of Fe-rich glassy slag. A) top view of 71139. B) top view of 71147:2. C) is characterized by fayalite (light grey phase), interstitial wüstite dendrites, metallic iron, and magnetite (light phase) embedded within glassy matrix (dark grey phase) on the top right. D) is a glassy slag mixed with charcoal and iron oxide zones at surface which are highlighted by red-dotted circles. E) is the optical photomicrograph of the red square in E) that is characterized by equiaxed magnetite, wüstite dendrites, and small amount of fayalite (light-grey phases) in glassy matrix, indicating a relatively oxidizing furnace condition. All optical photomicrographs were taken under plane polarized light, unless otherwise stated. (For interpretation of the references to colour in this figure legend, the reader is referred to the Web version of this article.)
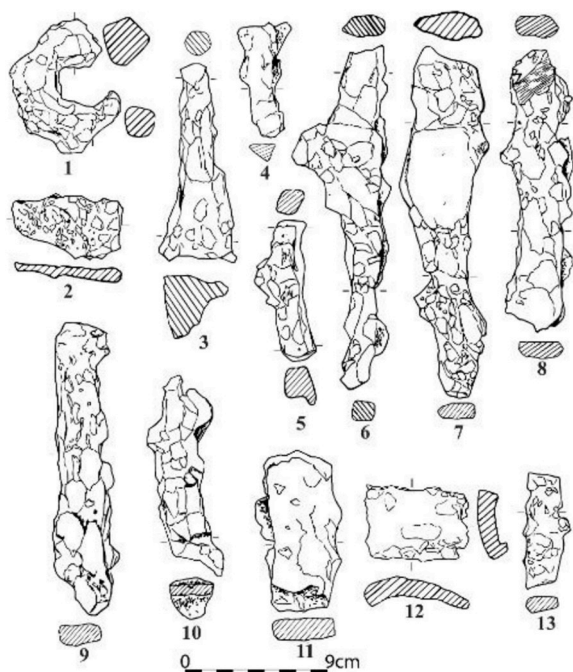
Fig. 5. Drawings of iron fragments sampled for metallurgical analysis.
(1. 71108; 2. 71203; 3.71117; 4. 71171; 5. 71119; 6. 71165; 7. 71148; 8. 71170; 9. 71290; 10. 71186; 11. 71126; 12. 71168; 13. 71174).

Fig. 6. Iron tools from the Taicheng cemetery selected for metallurgical analysis.
(1. sword 71300; 2. ring-pommeled knife 71306; 3. knife? 71314; 4. ring-pommeled knife 71315; 5. knife 71425; 6. ring-pommeled knife 71102; 7. ring-pommeled knife 71104; 8. ring-pommeled knife 71311; 9.cha-spade 71303; 10. ring-pommeled knife 71301; 11. ring-pommeled knife 71304; 12. Spade 71316; 13. ring-pommel knife 71105; 14. ring-pommeled knife 71313; 15. *ji*-halberd 71320; 16. sword 71424; 17. ring-pommeled knife? 71309).

since it can be contrasted with the "direct process" that reduced iron from ores directly by using a bloomery furnace.

Bulk chemical compositions and slag microstructure are both good indicators for distinguishing manufacturing waste from these processes. Cast iron smelting/melting would generate residues that were primarily in the form of a glassy matrix including sporadic cast iron droplets. Bloomery iron smelting slag, in contrast, is characterized by its glassy matrix, fayalite, and wüstite dendrites in addition to partially reduced ores and charcoal (Buchwald and Wivel, 1998; Huang et al., 2016;
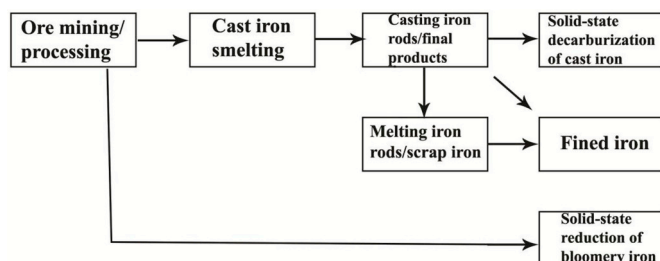

Fig. 7. *Chaîne opératoire* of iron manufacture and techniques in ancient China during the Warring States and Western Han period.

Gordon, 1997; Miller and Killick, 2004; Paynter, 2006). Microstructurally, fined iron (or finery) slag would have a glassy matrix with fayalite, wüstite, magnetite, metallic iron, and even cast iron (Huang et al., 2016; Gordon, 1997).

Criteria for identifying the steel-making techniques of products were proposed in the literature (e.g., Piaskowski, 1992; Rostoker and Dvorak, 1990). Solid-state decarburization of cast iron would result in products with very few if any SIs, unlike those made from bloomery iron and fined iron (Han and Chen, 2013, Wagner, 1993:291). Also, previous studies pointed out that the formation mechanisms of SIs in bloomery iron (direct process) and fined iron (indirect process) were different in several respects (Dillmann and L'Héritier, 2007, Han and Chen, 2013). During the finery process, due to thermodynamic reasons the P in cast iron will be firstly reduced and then appear in the α-Fe phase of iron as a P eutectic (Chen and Zhang, 2016, Huang, et al., 2016). In order to prevent the formation of iron phosphide in reducing environment, Ca-rich material (e.g., limestone) would be added to facilitate the formation of $3CaO.P_2O_5$, thereby eliminating the P content reduced in iron (Chen and Zhang, 2016; Dillmann and L'Héritier, 2007). In addition, P is more or less reduced depending upon the conditions inside the furnace. Previous studies comparing reference samples of known production technique showed that the percentage of P in trapped SIs from direct process steel was generally lower than that from indirect process (Dillmann and L'Héritier, 2007). Therefore, high Ca–P phases in SIs (in Chen and Zhang, 2016: 117, at least wt% CaO > 15%, P_2O_5 > 19%) can be a diagnostic characteristic for the identification of indirect process objects (Chen and Zhang, 2016; Han and Ke, 2007:614; Yang et al., 2014). Some other indicators, such as highly deformed SIs and the existence of "sub-double phase inclusions", in which SIs include fayalite and glass but do not display eutectoid phase separation as in double phase inclusions (Liu et al., 2014:60), have also been summarized in the previous discussion of potential differences between products and direct process (Chen and Zhang, 2016).

Nonetheless, the criteria mentioned above (high Ca–P phases as well as the size and shape of SIs) did not seem sufficient to fully differentiate fined iron (indirect process) from bloomery iron (direct process). For one thing, the chemical compositions of SIs are highly inhomogeneous due to the thermal condition insides furnaces, while SIs would also be deformed and fragmented because of the forging and welding process. Moreover, for objects that were made by fining but without adding Ca-rich flux, $3CaO.P_2O_5$ may not necessarily be identified in SIs trapped in final products (Chen and Zhang, 2016). Some smelting experiment analyses of SIs have shown that bloomery slag can contain up to 10 wt% P_2O_5 (Crew, 2000; Török and Thiele, 2013) if ores contain relatively high P. In terms of the shape and forms of SIs, previous studies (Wagner, 1993:294) have also suggested that the deformation and distribution of SIs could relate to the skill of smiths rather being solely contingent on manufacturing techniques.

In order to address the issues above, the statistical method developed by Disser et al. (2014), which was based on the ratio of non-reduced compounds (NRCs) including MgO, Al_2O_3, K_2O, SiO_2, CaO provides an important supplementary approach to process identification.

Table 2
Parameters of the logistic regression estimated based on 138 reference samples (From Disser et al., 2014: 328, Table 5).

Oxide**	Parameter	Value	Std.error
Intercept	β^0	5.22	3.320
MgO	β^{Mg}	0.13	0.35
Al$_2$O$_3$	β^{Al}	−0.95	0.25
SiO$_2$	β^{Si}	0.007	0.043
P$_2$O$_5$	β^{P}	0.16	0.065
K$_2$O	β^{K}	−0.84	0.44
CaO	β^{Ca}	0.088	0.058
MnO	β^{Mn}	0.018	0.091

Because of the relatively low temperature and incomplete reduction process, NRCs in SIs (average content determined by area-scanning) in bloomery iron objects came primarily from parent ores and the ratios of NRCs are relatively constant from ores to semi-products. In contrast, since NRCs from ores will mostly be removed during cast iron smelting, any NRCs in SIs formed through oxidization during the second stage of the indirect (or finery) process are primarily derived from furnaces, fluxes, and ashes. Consequently, SIs in indirect process products contained relatively small amounts of these compounds. In order to build a robust case using NRC ratios, Disser et al. (2014) developed a multivariate statistical method (Equation #1) based on the comprehensive mapping of SIs in the reference sets of 138 known samples and then calculated eight coefficients for their framework. Using the resulting eight parameters (Table 2), this multivariate statistical framework could compute a logit(p) for SIs and corresponding probabilities resulting from an indirect (p) or a direct (1-p) process for other unknown iron samples containing SIs.

Equation #1 (Disser et al., 2014:326, Equation 4)

$$\text{Logit}(p) = \beta^0 + \beta^{Mg}[\%MgO^{**}] + \beta^{Al}[\%Al_2O_3^{**}] + \beta^{Si}[\%SiO_2^{**}] + \beta^{P}[\%P_2O_5^{**}]$$
$$+ \beta^{K}[\%K_2O^{**}] + \beta^{Ca}[\%CaO^{**}] + \beta^{Mn}[\%MnO^{**}]$$

Logit(p): the result of the multivariate statistical study; β = Parameters of the logistic regression estimated based on 138 reference samples, see Table 2; %Oxide** = (%Oxide* × 100)/(100 − FeO*): ·%Oxide* = Average weighted compounds of SIs determined by area-scanning.

Although the logistic regression model was proven to offer an important and more objective approach for statistically differentiating between indirect and direct processes, it must be noted that the technological condition in ancient China might have differed from those in medieval France in a number of ways. For instance, the practice of iron recycling by welding multiple pieces of scrap iron together, which might lead to intensive forging and the concentration of some NRCs in SIs, has been often identified in the study of Han artifacts (Chen and Han, 2007). Moreover, when compared with cathedral clamps in medieval France, the manufacturing of high quality items such as swords with hundredfold refined layers (Wagner, 1993:282–284) which required greater working time, might create remarkable blurring effects caused by new SIs generated by hearth lining materials. These factors might have combined to increase the probability of misidentification, especially if the conditions at the testing facility did not allow intensive SEM-EDS mapping of all SIs to be carried out, as illustrated by the studies mentioned above (Disser et al., 2014). It remains to be seen whether the multivariate statistical method so successfully demonstrated on the medieval French materials can similarly be used to discriminate indirect and direct process products in ancient China, but this can be further tested by studies including larger groups of reference sets.

Given that these approaches have their own strengths and limitations, this research proposed to combine these methods together in order to make the identification results more robust (Table 3). To be

more specific, if multivariate statistical study of the average content of SIs indicates a high probability of indirect process, and point-scanning identifies that SIs include phases with relatively high Ca and P (i.e., CaO and P$_2$O$_5$ are both above 15 wt%) then the artifact can be reliably identified as a fined iron object. Also, for cases where the statistical analysis of bulk compositions of SIs does not show a high probability for either process (undetermined), but point-scanning suggests that high Ca−P phases exist in SIs, we propose that the example is possibly fined iron. If the result of the multivariate statistical study, which below we call logit(p), shows a high probability of direct process, and no high Ca−P phases were found, then the artifact is very likely made of the steel/wrought iron produced by the direct reduction of bloomery iron. However, if only high Ca−P phases or a logit(p) suggesting indirect process was identified, then the identification has to be carefully made on a case-by-case basis. For instance, if the logit(p) suggests that the sample was made by indirect process but no high Ca−P phases were found, this object might still have resulted from an indirect process as long as the evidence of flux addition (e.g., high content in MnO) is explicit and other NRCs that were primarily derived from ores (e.g., Al$_2$O$_3$) are relatively low. In contrast, when logit(p) suggests that the product was made by direct process but high Ca−P minerals were found, such objects should be viewed as undetermined, since how intensive reworking could impact on NRCs ratios is still unclear at this stage.

4. Results

4.1. Analysis of slag remains from the ironworks

After a careful examination of slag samples from dumping pits, their microstructures were confirmed in general to belong to three types: Si−Ca glassy slag, Fe-rich glassy slag, and furnace lining (Table 4). Twenty-eight samples were then selected for SEM-EDS analysis but as furnace lining data were unlikely to aid our understanding of manufacturing techniques, only the results of the first two types are reported below.

4.1.1. Si−Ca glassy slag

Microstructurally-speaking, this type of slag (Fig. 3A, Fig. 3B) was a glassy structure containing Si−Ca (or Si−Al) rich crystals and a few cast iron droplets. After etching, the iron globules often showed a two-phase structure comprising a P−Fe eutectic structure with high P wt% and a ferrite or pearlite structure (or ferrite) with low P wt% (Fig. 3C). Unmelted limestone and quartz particles (sand) were identified in six out of 28 SEM analyzed samples (Fig. 3D, Fig. 3E). In general, this type of slag should be related to the cast iron smelting/melting process (e.g., Chen, et al., 2011). Since no iron ores (or any ore-processing tools) were found in excavations at Taicheng, the archaeological context suggests that slag of this type is likely to be related to the melting process.

For iron melting in a cupola furnace or smelting in a blast furnace, slag is a necessary by-product of the process resulting from the addition of sand and flux to remove impurities from fuel ash or rusty scrap and to prevent oxidization of metallic iron. Meanwhile, adding limestone not only helps lower the melting point of slag but also reduce the loss of iron to slag (Rostoker and Bronson, 1990:104, Wagner, 2008: 36, 316). The discovery of unmelted limestone and quartz in this present case is likely to relate to the above processes, although some quartz particles might have been derived from the furnace lining material. In terms of chemical composition, this type of slag includes 52–58% SiO$_2$, 19–28% CaO, and 9–11% Al$_2$O$_3$ (supplementary Table: S1). The precentage of iron is consistently low in the chemical composition of slags, indicating that workers expertly controlled the reducing environment and the separation of slag and iron. The relatively high percentage of CaO and very low percentage of MgO suggest that limestone was used as flux to remove fuel ash and impurities.

Table 3
Identification standards of direct and indirect process employed in the article. ID: indirect process; D: direct process.

case	logit(p) shows a high probability of indirect process	logit(p) shows a high probability of direct process	logit(p) shows an undetermined stage	identification of high Ca−P phases in SIs	result
1	Y	–	–	Y	ID
2	–	Y	–	N	D
3	Y	–	–	N	ID
4	–	Y	–	Y	Undetermined
5	–	–	Y	Y	Possibly ID

4.1.2. Fe-rich glassy slag

The second type of slags examined included two samples (71139 and 71142:2, Fig. 4A, Fig. 4B). 71139 was identified as during the fieldwork because the surface texture and visual characteristics were different from common smelting/melting slag. The microstructure of 71147:2 shows components including iron oxide (magnetite), metallic iron, and a small amount of wüstite aggregated at the surface of the slag (Fig. 4C), together with a moderate amounts of unmelted quartz minerals in the glassy matrix. Sample 71139 is primarily a glassy slag with similar structure, including fayalite, wüstite, magnetite and aggregated metallic iron mostly near its surface (Fig. 4D, Fig. 4E). It must be noted that only part of these two samples consists primarily of iron oxides (magnetite/wüstite). Also, the area-scanning shows the glassy matrix of 71139 has relatively high CaO content, while the glassy matrix in sample 71147:2 was only high in SiO_2 (Table 5). In both samples, no high Ca−P phase was identified through SEM-EDS analysis, especially between dendrites of wüstite or iron oxide. The moderate amounts of iron oxide clustering in 71139 and 71147:2 indicate a rapid cooling and a change of relatively oxidizing conditions. One possible explanation is that the slag was related to a finery process, as is suggested by the relative oxidizing environment indicated. But given the fact that only two examples were found and microscopic features are not sufficiently diagnostic, it is difficult to exclude the possibility that these samples were formed when cast iron smelting/melting slag was oxidized and rapidly cooled down outside the furnace for some unclear reasons.

4.2. Analysis of iron fragments from the iron foundry

Table 6 shows the identification results of all samples and the number falling within each technical category. Not surprisingly, the majority of samples in the study (57 out of 107 analyzed samples) are either white cast iron, grey cast iron (the type of cast iron with carbon in the form of microscopic graphite flakse, see Wagner, 1993:344), or mottled cast iron (the type of cast iron showing a mixture of grey and white-cast microstructures, see Wagner, 1993:476). These cast iron samples could be either raw materials for melting/melting or, if their shapes are irregular, manufacturing waste (bear iron). In the assemblage, five samples out of the total 107 analyzed were identified as having large numbers of densely-packed and deformed SIs, which comprised either mostly glassy matrix containing iron oxides, or a mixture of iron oxides with other non-metallic intermediary phase compounds. These are very likely fragments of iron products or tools. Four of them, which included metallic bodies, were available for SEM-EDS analysis.

To further determine the techniques used in their manufacturing, area-scanning data of SIs in the four samples (Supplementary Table: S2)

were subject to the statistical analyses introduced above. As previous literature discussed (Disser et al., 2014), reduction (fining) was not always the major source of SIs; forge-inclusion, welding, and fluxing adding can all contribute to the fragmentation of SIs in the metallic body or the creation of SIs that are not related to the reduction/finery process. Therefore, area-scanning data must firstly be subjected to treatment using statistical method in order to eliminate blurring effects not related to reduction/fining.

The treatment procedures for 71119 (Fig. 8A) followed those outlined before and are explained below as an illustration for all other samples. Since P_2O_5 and FeO can be concentrated and are prone to impacts during heat-treatment, and NRCs (MgO, Al_2O_3, K_2O, SiO_2 and CaO) are relatively stable, the values of these five oxides were transformed into log-ratio data (XiNRC) following the Equation proposed by Disser et al. (2014: 324, Equation (2)) in order to facilitate sub-compositional standardization. The XiNRC data were then submitted to a hierarchical cluster analysis based on Euclidian distances using the Ward method for R-packages. The discrimination threshold was chosen to cut the dendrogram tree in order to obtain four groups of SIs (Fig. 9). The results of clusters are plotted again using principal component analysis (PCA) scores performed on XiNRC in order to verify the validity of grouping (Fig. 9). As the ratio of NRCs that came directly from the reduction/fining stage should, theoretically, remain constantly and comparably in SIs (Dillmann and L'Héritier, 2007; Disser et al., 2014), the grouping results can then be plotted on bivariate graphs using mass % of Al_2O_3, SiO_2, CaO, K_2O, and MgO as parameters to determine the groups that are more likely to be related to the reduction/fining stage. In the case of 71119, cluster 3 is considered to be closely related to reduction/fining because the values are more concentrated and aligned towards the zero point (Fig. 10).

After the first treatment, the area-scanning data of cluster 3 in 71119 was analyzed using the multivariate framework (Disser et al., 2014) (Table 7). To avoid any disturbance due to matrix effects (i.e., over evaluation of the Fe content), we follow the additional step proposed by Disser et al. (2014:325) to calculate a new compositional ratio (%Oxide**) for each oxide except iron before applying the logistic regression model. The results show that, with high probability, this sample should have been produced by the indirect process (Table 7). In Table 8, we also list the frequencies of points where high wt% of both CaO and P_2O_5 (i.e., Ca−P phases) were recorded. According to the result, high Ca−P phases are commonly found in this sample; indeed some of them are even higher than 20%. Given the probability indicated by the logistic regression model and the identification of $3CaO.P_2O_5$, this sample matches the criteria for fined iron.

As sample 71117 (Fig. 8B) was made by welding and included at least four layers (below we will use "zone" to indicate each of these

Table 4
Identification result of analyzed slag samples.

	Glassy slag	Mixture of slag, iron and charcoal fragments	Other	Total analyzed	SEM-EDS analyzed
Smelting/melting slag	26	22		48	22
Furnace lining	9	8	1	18	4
Fe-rich glassy slag		1	1	2	2

Table 5
Chemical compositions of Fe-rich glassy slag through area scanning (wt%). N.d. means no observable peak distinguishable from background noise. "*" after the average chemical composition represents that it is below the detection threshold. Sum different of 100 because of some minor elements not presented in this table.

Sample #	Feature	Na$_2$O	MgO	Al$_2$O$_3$	SiO$_2$	P$_2$O$_5$	K$_2$O	CaO	MnO	FeO
71139	Glassy matrix	1.1	0.9	14.1	63.5	3.5	6.3	7.2	0.3	1.7
71139	Glassy matrix + magnetite	1.3	1.1	14.7	59.5	3.5	6.2	8.9	0.2	2.4
71139	Glassy matrix + magnetite	1.1	2.1	11.0	57.6	3.2	4.3	12.6	0.2	6.8
71139	Glassy matrix	0.9	2.7	9.5	56.0	2.3	4.3	23.4	0.1*	0.5
71139	Glassy matrix	1.4	0.7	16.7	57.9	3.6	7.8	6.8	0.6	1.8
71139	Magnetite + fayalite + small amount of glassy matrix	0.8	1.9	8.2	33.9	3.4	1.3	4.6	0.3	44.2
71147:2	Metallic iron + fayalite + matrix	0.3	0.4	2.6	15.8	2.1	0.6	1.7	0.3	75.8
71147:2	Fayalite + matrix + magnetite	0.7	0.6	4.4	37.5	2.2	1.3	2.5	0.2	50.3
71147:2	Grassy matrix + magnetite + wüstite	1.3	0.9	7.9	49.5	1.7	2.3	2.7	0.2	33.0
71147:2	Fayalite + glassy matrix	0.9	1.0	5.1	39.8	2.3	1.4	4.0	0.3	44.7
71147:2	Fayalite + glassy matrix	0.7	0.8	4.6	32.8	2.9	1.2	3.6	0.2	53.1
71147:2	Glass matrix (with unmelted quartz)	0.8	0.8	9.2	76.7	1.4	4.1	1.1	n.d.	5.3

layers that can be separated by welding lines and different carbon contents) of blooms with various carbon contents, slightly different pre-treatment was adopted for this type of samples. First, the data for all collected SIs were plotted on bivariate graphs using mass% of Al$_2$O$_3$, SiO$_2$, CaO, K$_2$O, and MgO (Supplementary Figure: S1). The result shows that, chemically, SIs in zone 1 and zone 2 appear to be distinctively different from SIs in zone 3 and zone 4, which means these layers came from different reduction/finery systems or received different degrees of impact from welding. Since zone 1 and zone 2 include relatively few SIs for analysis (Fig. 8B), SIs in the first two zones are grouped together for comparison with the results in zone 3 (zone 4 is excluded here as SIs are very few). Second, SIs of these two large groups (zone1/2 and zone 3) were then subjected to hierarchical clustering and PCA respectively, and the results were again plotted on bivariate graphs, similar to the process for 71119, in order to identify which cluster could be related to reduction (fining) processes. Table 7 lists the logit(p) of the two large groups. While the data of zone 3 suggested an undetermined nature, those from zones 1 and 2 may be related to direct processes (Table 7). However, high Ca−P phases were commonly found in both these two major groups. Here it must be noted that zones 1 and 2 are external layers in this welded sample. Some SIs in these two layers also include relatively high SiO$_2$ content (Supplementary Figure: S1), indicating they were likely to be impacted by forging processes. Therefore, we would identify zone 1 and zone 2 as undetermined, and zone 3 as possibly a piece of fined iron.

Table 7 presents the values of logit(p) and corresponding probabilities in order to predict the techniques of other two samples with SIs (71121 and 71126; for details of identification, see Supplementary Table: S3) found at Taicheng. The calculation of logit(p) and treatment of SI data are similar to the illustration for 71119 described above. There is a high probability that these two samples were manufactured by indirect process. Moreover, high levels of Ca−P phases were identified in SIs in sample 71121 (Fig. 8C) and 71126 (Table 8). Based on these combined results, we identified these two samples as fined iron objects.

In the assemblage, there are seven samples that can be categorized as steel made by solid-state decarburization of cast iron (Fig. 8D, Fig. 8E, Supplement Table: S3). Among them, two samples might have been semi-products (iron rods), which was suggested by their thick, bar shape and lack of edges (Fig. 5.8 and 5.9). In addition, two pieces of malleable cast iron (Fig. 8F) were found in this study. One of them,

71168, was a fragment with curved profiles (Fig. 5.12), which might have been part of a vessels. Some C-shaped or S-shaped (Fig. 5.1) artifacts (in plan) were also identified as steel made by solid-state decarburization of cast iron, thus paralleling discoveries made in previous metallurgical studies (e.g., Chen, 2014: 279–287, Liu et al., 2014), which found that ring-pommeled knives were made primarily of this type of material.

Besides iron pieces from excavated features, our project also recovered micro-remains that are very likely to be hammer scale (Fig. 11). Given that this type of material is often found surrounding a smithing hearth (Sim, 1988; Veldhuijzen and Rehren, 2007), the discovery provides our best evidence of iron forging. The material's microstructure revealed complete corrosion, but the layering of Fe$_2$O$_3$ and Fe$_3$O$_4$ was still clearly observable, which is indicative of the oxidized surface layer of an iron object that falls off during the hammering procedure.

4.3. Iron products from the Taicheng cemetery

The metallurgical study of iron objects from the cemetery offered supplementary results for the study of ironworks. The 18 identifiable samples (Table 9; for details, see Supplementary Table: S4) include one of malleable cast iron, 11 pieces of steel/wrought iron made by solid-state decarburization of cast iron (Fig. 12A, Fig. 12B), and six objects with large amounts of SIs. Based on the available samples, it seems that solid-state decarburization of cast iron was the primary material used on site for manufacturing iron tools and weapons. Although bar-shaped steel objects found in rubbish pits could have been used for this purpose (71170, see Fig. 5.8), no casting molds for making knives or rods were found during the excavations.

Six of the samples include large amounts of SIs and thus can be identified as either fined iron products or bloomery iron from solid-state reduction. Based on the bulk chemical compositions (Supplementary Table: S2) and microscopic structure, we describe the identification results in terms of two categories.

4.3.1. Products related to indirect process

This cateogory comprises samles 71304, 71316, and 71320. Micrographically, 71304 was made from one piece of steel. In this sample, the SIs relating to reduction/fining (Cluster 3 & 4) produced an "undertermined" result because of the low probability of logit(p)
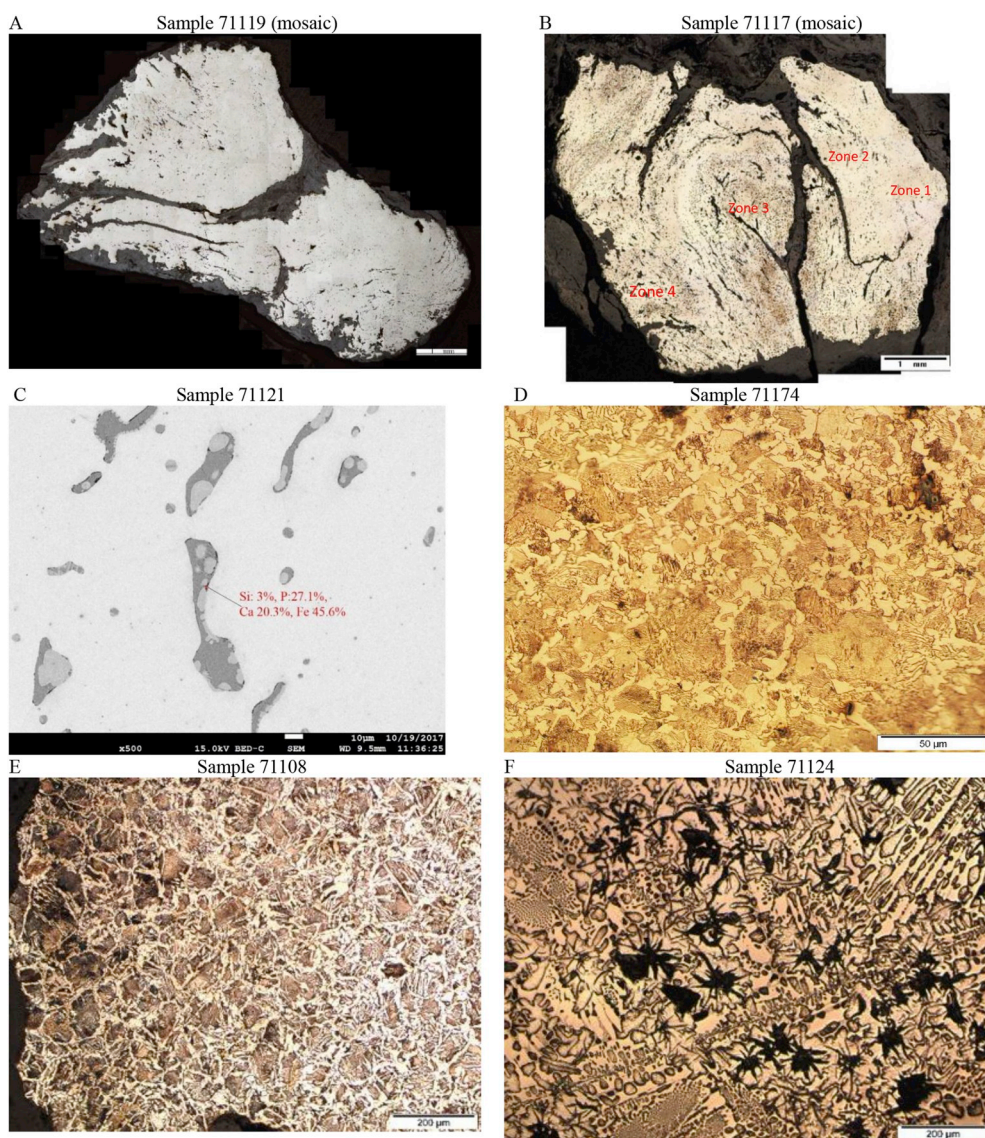
Table 6
Results of metallurgical identification of iron pieces from the ironworks.

	Cast iron	Solid-state decarburization of cast iron/malleable cast iron	Fined iron/Welded object made of fined iron	Wrought iron	Completely corroded	Total
Potential iron tools	25	6	5	11	9	56
Unidentifiable iron objects	32	4		5	10	51

Fig. 8. Optical photomicrographs and SEM image of selected iron samples from the ironworks. A) is characterized by ferrite includes elongated and deformed SIs. B) shows a U-shape cross-section that was welded by at least 4 layers of wrought iron with highly deformed SIs. C) is a SEM (backscattered) image of a SI in 71121. The light phase in SI is iron oxide, and grey phase is a glassy matrix. At the edge of iron oxide, dark-phases were identified (red arrow) with relatively high wt% CaO and P_2O_5. D) shows pearlite + ferrite (hypo-eutectoid steel). E) shows pearlite + ferrite with widmanstätte structure. F) shows the microstructure of malleable cast iron characterized by ledeburite and unevenly distributed nodular graphite. (For interpretation of the references to colour in this figure legend, the reader is referred to the Web version of this article.)

(Table 7). However, as high Ca–P phases were also identified (Table 8), we would suggest that this sample is possibly an indirect process product. The other two samples, 71316 and 71320 (Fig. 12C) were made by welding at least two pieces of wrought iron or steel together. In the two-layer structure of 71316, one layer (zone 1) had dense SIs, while the other (zone 2) had very few (Supplementary Figure: S2). The latter layer might be steel made by solid-state decarburization of cast iron. The former layer with trapped SIs has a high probability of being steel made by indirect process (Table 7). As high Ca–P phases were also found in this example (Table 8), the object was made by welding together at least one piece of steel made by solid-state decarburization of cast iron and one piece of fined iron. In addition, the ratios of NRCs in the SIs of 71304 is similar to those of one fined iron (71119) from the ironworks (Supplementary Figure: S4). One possible explanation is that these fined iron objects recovered from the ironworks and cemetery might have been manufactured using simialar finery systems or at the same site. In cross-section of 71320, the high-carbon zone (ferrite + pearlite) appears to "wrap" the low-carbon zone (ferrite) as the pieces of wrought iron were folded several times. The ratios of NRCs in bivariate plots shows that SIs in the two zones cannot be clearly separated (Supplementary Figure: S3). The SIs from the two zones were therefore grouped together for Ward analysis in order to identify clusters for regression analysis, which indicated a high probability that

71320 was made by indirect process (Table 7). Also, the SIs in this sample were characterized by high MgO contents, which might have been added as flux rather than being derived from the partent ores given the low Al_2O_3 content. Therefore, despite the absense of high Ca–P phases (Table 8), we would nevertheless suggest that this smaple is probably from a fined iron object. Also, the production site of this sample may even be different from that of other found fined iron objects.

4.3.2. Products related to direct process or undetermined

This group comprises sample 71309, 71412, and 71420. Of these, 71309 and 71412 were made by welding multiple pieces of steel/wrought iron together. In the two-layer structure of 71309 (Fig. 12D), only one layer (zone 1) includes dense SIs should be related to fining/reduction processes. There are only very few minute SIs in zone 2, and they are characterized by a high SiO_2 glassy matrix (Supplementary Figure: S5). The latter might primarily be derived from the forging process and were therefore excluded from our calucation. Nonetheless, there were no high Ca–P phases found by point-scanning in SIs analyzed throughout the sample (Table 8). The probability indicated by the logit(p) of zone 1 suggests that this part of the sample is very likely to be a direct process product (Table 7). Sample 71412 was also made by welding together two pieces of wrought iron (zone 1 and 3) and one
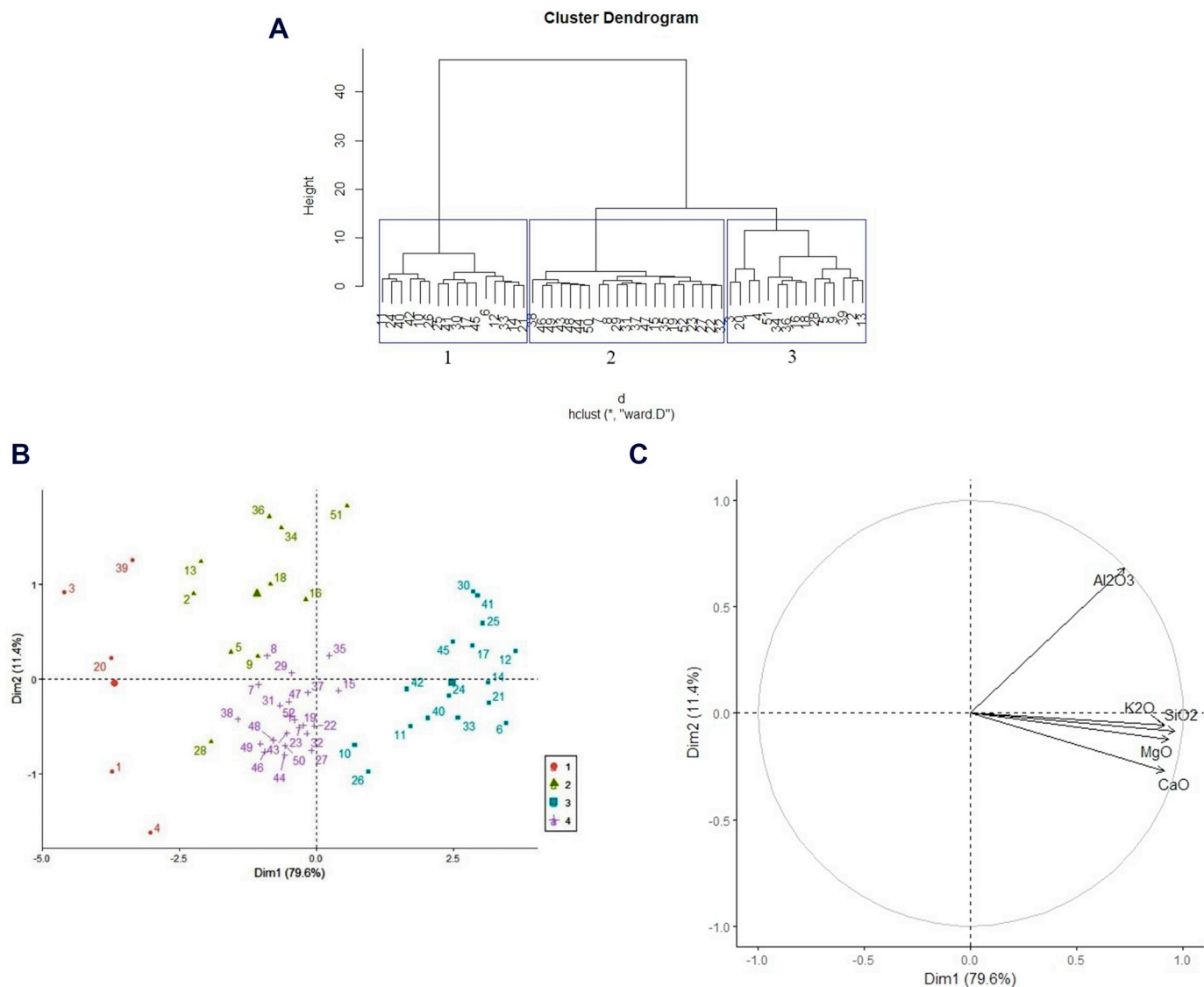
Fig. 9. Pre-treatment of chemical compositions of SIs in 71119 employing statistical methods. A: Dendrogram of hierarchical clustering of XiNRC in 71119 following the Ward Method and instructions as presented in Disser et al., 2014. B and C: PCA of SIs based on the groupings by Ward Method.

piece of steel (zone 2) (Fig. 12E; for NRCs ratios, see Supplementary Figure: S6). Zone 1 and 3 were the surface parts of the sample and included only small amounts of SIs, while the center of the cross-section, zone 2, included dense SIs suitable for Ward analysis. The logit(p) of zone 2 indicates a high probability of direct process manufacturing (p < 0.01) (Table 7). However, high Ca—P phases were identified in some trapped SIs (Table 8). Similarly, the logit(p) of SIs in 71420 also indicated a high probability of direct process, while high Ca—P phases were commonly found in SIs (Tables 7 and 8). Since it is unclear in these two cases to what extent the ratio of NRCs in SIs would be blurred by heavy forging and welding process, we regard both 71412 and 71420 as undetermined.

In sum, with the exception of the undetermined cases, the results of metallurgical analyses revealed a variety of materials and manufacturing techniques used in the production of tools, which might indicate that they came from various sources.

5. Discussion

5.1. Manufacturing techniques at the Taicheng ironworks

The analytical results of samples of manufacturing waste from Taicheng ironworks have helped clarify several aspects of the manufacturing process and its products. The microstructure and chemical composition of smelting/melting slag have confirmed that casting was the primary technique employed at the site. The discovery of incompletely melted limestone and the relatively high content of CaO in the glassy matrix of slags shows that limestone was used as a flux. The iron foundry might also have engaged in small-scale fined iron production alongside cast iron manufacturing. However, the very limited evidence identified during the systematic sampling and insufficiently diagnostic character of the two samples' optical microstructure prevent us from confidently identifying them as samples made using a finery
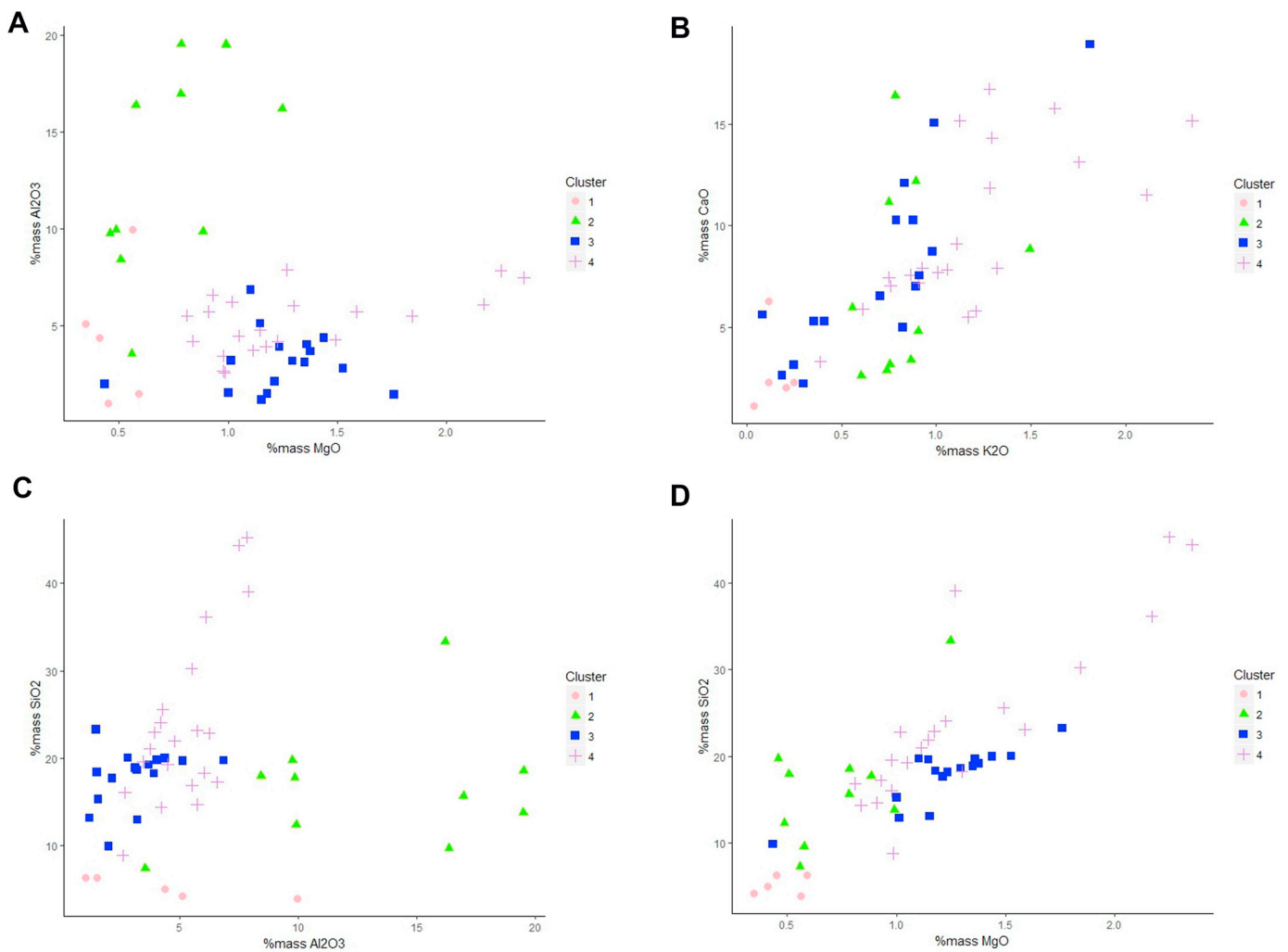
Fig. 10. Bivariate plots of various NRC couples in SIs of sample 71119 according to Ward grouping result in Fig. 9.

process. Therefore, the question of whether small-scale ironworks like Taicheng would occasionally have conducted finery processing will have to await confirmation once additional empirical evidence has been collected from similar types of ironworks in the future. The identification of hammer scale also confirmed the existence of smithing activities,

although it is unclear whether it was related to tool manufacturing or repairing. In short, metallurgical evidence shows that even though cast iron melting was the major production method, other manufacturing skills were also employed by workers at the ironworks.

Table 7
Average chemical compositions (wt%) of the cluster of SIs in samples with dense SIs for multivariate statistical analysis and prediction of iron-making process for samples from the ironworks and cemetery based on logit(p). Detection limit was empirically determined to be 0.1 wt%. "*" after the average chemical composition represents that it is below the detection threshold. For original data see Supplement Table: S2.

Sample #	Zone and cluster in Ward	MgO*	Al_2O_3*	SiO_2*	P_2O_5*	K_2O*	CaO*	MnO*	FeO*	Logit (p)	Probability of indirect process	Probability of direct process	Identification based on logit(p)
71117	zone 3 (cluster 3&4)	0.55	6.48	7.76	19.30	0.50	9.15	0.33	52.28	−0.74	0.32	0.68	Undetermined
71117	zone 1&2 (cluster 1 & 4)	1.27	6.23	24.48	9.06	0.90	12.39	0.65	43.37	−4.14	0.02	0.98	Direct process
71119	cluster 3	1.22	3.14	17.79	15.77	0.70	7.85	0.30	50.85	5.08	> 0.99		Indirect process
71121	cluster 3	0.40	0.84	5.91	14.29	0.32	4.41	0.24	72.26	11.27	> 0.99		Indirect process
71126	cluster 2 & 3	0.44	2.37	3.08	25.14	0.10*	2.72	0.37	61.42	11.24	> 0.99		Indirect process
71304	cluster 3 &4	1.28	5.59	26.21	11.26	0.89	7.77	1.01	43.26	−0.24	0.44	0.56	Undetermined
71309	zone 2 (cluster 2)	1.89	8.36	19.99	0.76	0.42	2.04	1.46	63.73	−13.35		> 0.99	Direct process
71316	zone 1 (cluster 1 & 3)	0.50	2.35	7.46	15.68	0.47	4.17	0.42	68.14	4.24	0.99		Indirect process
71320	cluster 1	0.24	0.08*	45.21	0.43	2.01	0.38	35.84	14.27	6.48	> 0.99		Indirect process
71412	zone 2 (cluster 3 & 4)	0.74	4.85	17.77	2.98	1.54	8.17	0.09*	63.27	−7.066		> 0.99	Direct process
71420	cluster 4	1.19	7.21	15.21	13.27	1.04	19.25	0.37	40.41	−2.66	0.07	0.93	Direct process

Table 8
Counts of SEM-EDS points in SIs with high wt% P₂O₅ and wt% CaO.

Sample #	Total points of spots (in phases or crystals) analyzed by SEM-EDS	wt% P₂O₅ and wt% CaO ≥ 15%	wt% P₂O₅ and wt% CaO ≥ 20%	Final identification result
71117(zone 3)	89	19	13	Possibly ID
71117(zone 1&2)	43	12	4	u.d.
71119	124	33	28	ID
71121	69	7	4	ID
71126	47	1	0	ID
71304	88	18	13	Possibly ID
71309(zone 2)	87	0	0	D
71316(zone 1)	64	9	7	ID
71320	88	0	0	ID
71412(zone 2)	190	9	6	u.d.
71420	128	27	16	u.d.

(ID: indirect process; D: direct process; u.d.: undetermined).

5.2. Raw materials and potential products of the ironworks

The study of iron fragments indicates that a wide range of raw materials were collected for use in production. The four samples identified as fined iron, or which used fined iron as their raw material, should each be a fragment of some kind of tools. Also, some curved fragments of iron vessels and broken pieces of ring-pommeled knives were found in the assemblage. But scrap iron alone could not satisfy the raw material needs of the ironworks. Among the samples identified as solid-state decarburization of cast iron are two special rectangular, thick bar-shaped objects that are very likely to be semi-products. Molds for casting this type of iron bars were found at other large-scale excavated iron foundries (Henan, 2007; Li, 1995), but not at Taicheng. The systematic sampling of iron fragments has shown that small-scale ironworks such as Taicheng might have procured semi-products or raw materials through exchange, which is a system that has not been considered before in the literature.

5.3. Techniques of products from the nearby cemetery

By synthesizing metallurgical and typological analyses, the study of manufacturing techniques has confirmed that the major types of artifacts recovered from the nearby cemetery were manufactured using a variety of different techniques including solid-state decarburization of cast iron, fined iron, and potentially bloomery iron. Some objects, however, might not even have been made by the Taicheng ironworks. As mentioned above, no vessel casting molds were identified during the entire excavation, which therefore indicates that the vessels found in the cemetery must have been procured via exchange. The one object potentially made of bloomery iron is also unlikely to be manufactured by the ironworks, although the provenience of this piece is yet to be

Table 9
Results of metallurgical identification of iron pieces from the cemetery.

Types	Numbers
Steel made by solid-state decarburization of cast iron	11
Malleable cast iron	1
Fined iron	1
Welded fined iron	1
Welded fined iron and solid-state decarburization of cast iron	1
Probably bloomery iron	1
Wrought iron/steel with SIs but the manufacturing process cannot be determined	2
Unidentifiable because of corrosion	5

clarified. Metallurgical analyses revealed that ring-pommeled iron knives, the major type of tools in the funeral assemblage, were made of solid-state decarburization of cast iron. Given the complete absence of molds for casting iron rods at the foundry, the analyses of cemetery objects imply that most artifacts found in burials might not have been made entirely at Taicheng. One can argue that the ironworks might have contributed some tools to the funeral assemblage through smithing scrap iron or forging imported semi-products (e.g., iron rods). However, the lack of evidence for large-scale manufacturing of semi-products (e.g., casting molds for iron rods) or fined iron together indicate that the procurement of the raw materials needed to sustain iron production and the manufacturing of final iron products to support daily life might have, to a large extent, relied upon external exchange.

5.4. "Small-scale" ironworks and the iron industry in the Han capital region

The Taicheng ironworks appeared to be a small, local production center making limited types of agricultural tools. However, the results of comparative analyses suggest that the Taicheng cemetery yielded a large number of iron goods that could not be directly manufactured by the neighboring ironworks. Based on previous archaeological investigations (see synthesis in Bai, 2005, 396–397), no other large-scale ironworks that could manufacture cast iron knives, vessels, and iron bars has yet been discovered inside the Wei River Valley; indeed, most of them were similar to the Taicheng ironworks in terms of scale and assemblage. Even where the procurement and supply of iron raw materials was concerned, the issue could not be addressed solely by the recycling of scrap iron; it must rely on an exchange system to a certain extent (Lam et al., 2015), no matter whether the network was controlled by the state or run by private entrepreneurial merchants. Therefore, by drawing upon metallurgical analyses and comparison of manufacturing remains from different contexts, this study argues that the procurement of raw material resources, supply of finished products, and techniques employed in local ironworks like Taicheng must all be reconsidered. Even though the extent to which the production and
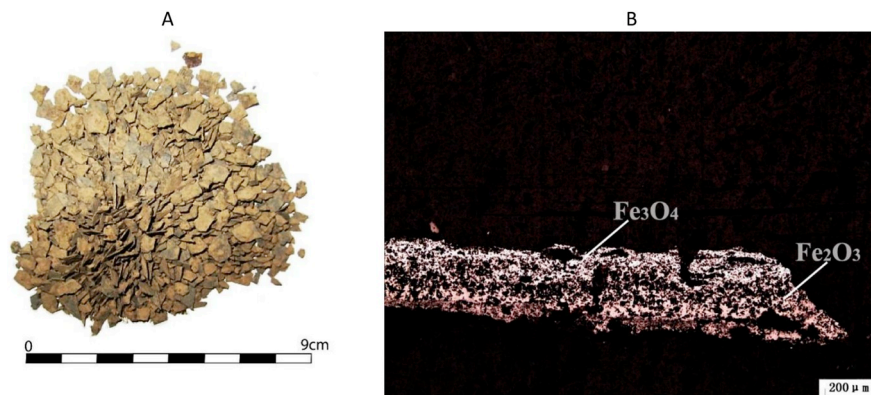

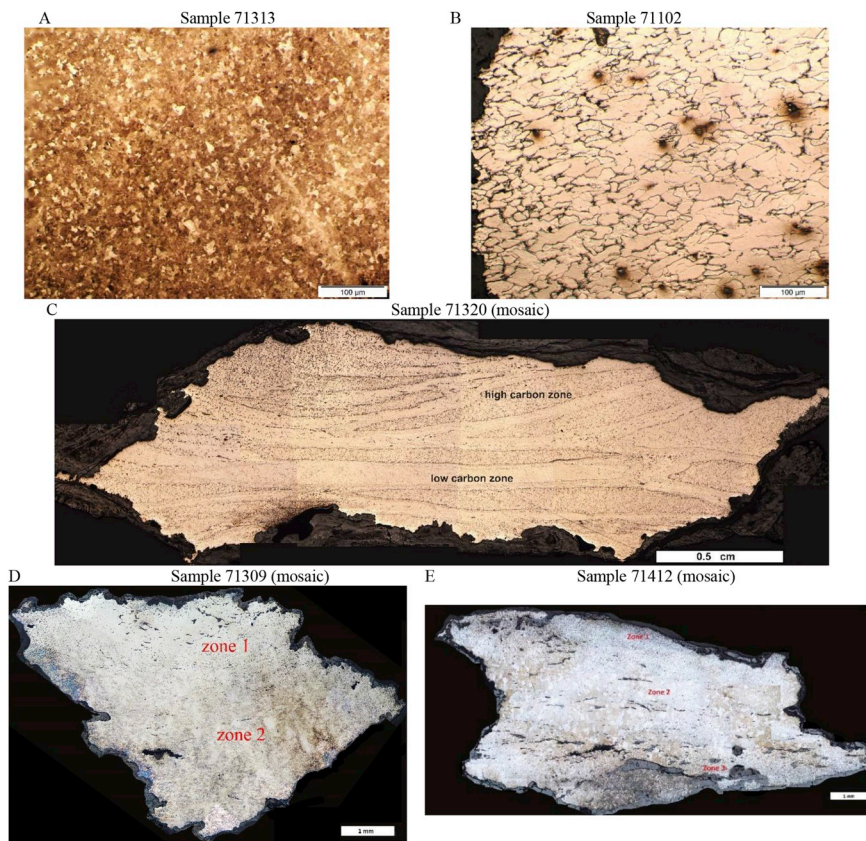**Fig. 11.** Hammer scale and its photomicrography.

Fig. 12. Optical photomicrographs of iron objects from the Taicheng cemetery. A) shows pearlite + ferrite. B) shows ferrite + few pearlite with very few SIs. C) shows high carbon zone was "wrapped" by low carbon zone as these two pieces of wrought iron were folded several times after they were welded. Both zones contained deformed SIs, and ratios of NRCs in bivariate plots from these two zones are similar to a certain extent. D) shows a welding structure. Zone 1 is ferrite with few pearlite containing relatively dense SIs. Zone 2 shows pearlite with ferrite but only includes few glassy SIs. E) is characterized by three-layer structure. Zone 1 and zone 3 are primarily ferrite with very few SIs, while the central part (zone 2) is pearlite + ferrite with deformed SIs.

consumption was managed by the Han government is still debatable, the management of the Taicheng iron industry must involve, at least partially, interregional exchange and transportation to secure the supply of raw materials or finished products for the local community.

6. Conclusion

Until recently, the study of the Han iron industry focused primarily on large-scale ironworks. The analysis of remains from a small ironworks and its nearby settlement in this case offered valuable information that has been ignored before, which in turn yielded several new insights. It was confirmed that small ironworks in the headquarters region relied upon the recycling of scrap iron as raw materials. But the role of exchange should not be overlooked. Such ironworks might procure semi-finished products for the manufacturing of finished products via hammering. Local recycling and importation through exchange both played a key role in the iron-related economic system. Nonetheless, this small ironworks could only address the demands for agricultural tools and, potentially, small numbers of other tools. Within the Taicheng site complex, certain iron products important in daily life were not made by the local ironworks and still required imports from other workshops probably outside the capital region. Therefore, the study of slag and iron remains suggest that the Taicheng ironworks and its nearby community employed a "diversification" strategy in order to maximize the sources of raw materials and supplies of finished product. In reality, this ironworks and the nearby community were supported by both an internal system aimed at recycling materials from nearby settlements and an external system used to procure goods via a large-scale exchange network. The combination of local production and intensive exchange network provided the essential foundation for the prosperity and thriving development of iron economies during the Han period. In sum, the comparison of metallurgical analyses between manufacturing and consumption sites holds promise to shed light on a macro-scale picture of the Han iron industry and the interaction between craft production and political infrastructure.

Appendix A. Supplementary data

Supplementary data to this article can be found online at https://doi.org/10.1016/j.jas.2018.09.009.

References

Bai, Y., 2005. Archaeological Study on Iron Works before 3rd Century A.D. In China (先秦两汉铁器的考古学研究). Science Press, Beijing.

Beijing [Beijing keji daxue yajinshi yanjiushi], 1996. Metallurgical report on the analysis of iron objects from the Jiaoliu architectural site (角楼建筑遗址出土铁器金相鉴定报告). In: Institute of Archaeology, Chinese Academy of Social Sciences (Eds.), Weiyang Palace in Han Chang'an city: 1980-1989 Excavation Report, [长安城未央宫:1980-1989年考古发掘报告]. Zhongguo Dabaike Quanshu Press, Beijing, pp. 269.

Buchwald, V.F., Wivel, H., 1998. Slag analysis as a method for the characterization and provenancing of ancient iron objects. Mater. Char. 40, 73–96.

Chen, J., 2014. Exploration of the Metal Smelting and Casting Civilization in Ancient

China (中国古代金属冶铸文明新探). Science Press, Beijing.

Chen, J., Han, R., 2000. Comparative studies on iron and steel artifacts unearthed from the tombs of Han princes (汉诸侯王陵墓出土铁器的比较). Sci. of Conserv. Archaeol 12, 1–8 文物保护与考古科学.

Chen, J., Han, R., 2007. Iron and Steel Technology in Central Plains and Northern Region during the Han and Jin Dynasties (汉晋中原及北方地区钢铁技术研究). Beijing Daxue Press, Beijing.

Chen, J., Zhang, Z., 2016. Identification of ancient cast iron-fining technology based on slag (基于炉渣分析的古代炒钢技术判定问题). South. Cult. Relics 1, 115–121 南方文物.

Chen, J., Hong, Q., Qin, Z., Liu, H., Han, R., 2011. Preliminary study on the smelting and melting techniques based on remains from the Wanchenggang iron production site, Lushan (鲁山望城岗冶铁遗址的冶炼技术初步研究). Huaxia Archaeol 3, 99–108 华夏考古.

Crew, P., 2000. The influence of clay and charcoal ash on bloomery slags. In: Tizzoni, C.C., Tizzoni, M. (Eds.), Iron in the Alps: Deposits, Mines and Metallurgy from Antiquity to the XVI Century, Bienno, pp. 38–48.

Dillmann, P., L'Héritier, M., 2007. Slag inclusion analyses for studying ferrous alloys employed in French medieval buildings: supply of materials and diffusion of smelting processes. J. Archaeol. Sci. 34, 1810–1823.

Disser, A., Dillmann, P., Bourgain, C., L'Héritier, M., Vega, E., Bauvais, S., Leroy, M., 2014. Iron reinforcements in beauvais and metz cathedrals: from bloomery or finery? The use of logistic regression for differentiating smelting processes. J. Archaeol. Sci. 42, 315–333.

Du, F., Han, R., 2005. Identification of iron objects from the arsenal site in Han Chang'an (汉长安城武库遗址出土部分铁器的鉴定). In: Institute of Archaeology, Chinese Academy of Social Sciences (Eds.), The Arsenal Site in Han Chang'an, [汉长安城武库]. Cultural Relics Press, Beijing, pp. 132–133.

Du, N., Li, J., Chang, G., Wan, X., Li, Y., 2011. Survey and research on iron production sites in northeastern capital city of the Qi state in Linzi, Shandong (山东临淄齐国故城东北部冶铁遗址的调查与研究). J. Jiangxi Univ. Sci. Technol 32, 12–15 江西理工大学学报.

Du, N., Li, Y., Zhang, G., Wang, X., Li, J., 2012. Studying on ancient iron smelting relics in the south of the capital city Linzi (临淄故城南部炼铁遗物研究). China Min. Magazine 21, 115–120 中国矿业.

Gordon, R.B., 1997. Process deduced from ironmaking wastes and artefacts. J. Archaeol. Sci. 24, 9–18.

Guo, M., Chen, K., Mei, J., Sun, Z., Shao, J., Shao, A., 2014. Scientific analysis of iron objects from the Zhaitouhe cemetery in Huangling, Shaanxi (陕西黄陵寨头河战国墓地出土铁器的初步科学分析研究). Archaeol. and Cult. Relics 2, 121–127 考古与文物.

Han, R., Chen, J., 2013. Casting iron in ancient China. In: Humphris, J., Rehren, T. (Eds.), The World of Iron. Archetype publications, London, pp. 168–177.

Han, R., Duan, H., 2009. An early iron-using center in the ancient jin state region (8th-3rd century BC). In: Mei, J., Rehren, T. (Eds.), Metallurgy and Civilisation: Eurasia and beyond: Proceedings of the Sixth International Conference on the Beginnings of the Use of Metals and Alloys (BUMA VI). Archetype Publications, London, pp. 99–106.

Han, R., Ke, J., 2007. China Science and Technology History (Volume of Mining and Smelting) (中国科学技术史(矿冶卷)). Science Press, Beijing.

Henan [Henansheng wenwu kaogu yanjiusuo], 2007. The Sacrificial Site of the Zheng State in Xinzheng (新郑郑国祭祀遗址). Daxiang Press, Zhengzhou.

Henan, Lushan [Henansheng wenwu kaogu yanjiusuo, Lushanxiang wenwu guanli weiyuanhui], 2002. Preliminary report on the excavation of the no.1 furnace at the Wangchenggang site, Lushan (河南鲁山望城岗汉代 冶铁遗址一号炉发掘简报). Huaxia Archaeol 3, 3–11 华夏考古.

Huang, Q., Li, Y., Chen, J., Tie, F., 2016. A summary of ancient iron smelting technology based on iron slag analysis (以炉渣分析为主揭示古代炼铁技术的研究与探索). J. Natl. Mus. China 11, 145–153.

Kageyama, T., 1984. Iron handicraft and monopoly in ancient China (中国古代の製鐵手工業と專売制). In: Industry, Business, and Monopoly in Ancient China, [古代の商工業と專売制]. Tokyo University Press, Tokyo, pp. 271–309.

Lam, W., 2014. Everything old is new again? Rethinking the transition to the cast iron production in the Central Plains of China. J. Anthropol. Res. 70, 511–542.

Lam, W., Chen, J., Chong, J., Lei, X., Zhao, Y., Chen, G., 2015. On the provenience and circulation of raw materials for iron production in the guanzhong area of the Han

period: a case study of iron remains identified from the Taicheng foundry (试论汉代关中地区铁器生产原料的来源与流通—邰城铸铁作坊出土铁遗物的冶金分析). Archaeol. Cult. Relics 6, 95–109 124, 考古与文物.

Li, J., 1995. Iron Production during the Han Period in Nanyang (南阳汉代冶铁). Zhongzhou Guji Press, Zhengzhou.

Liu, C., 1999. Spectrum and microstructure analysis of metal objects from early Western Han tombs in Longshouyuan (龙首原西汉早期墓出土金属器件的能谱及金相显微组织分析). In: Xi'an Municipal Institute of Cultural Relics Conservation and Archaeology (Ed.), Western Han tombs in Longshouyuan, Xi'an, [西安龙首原汉墓]. Xibei University Press, Xi'an, pp. 262–270.

Liu, H., Chen, J., Mei, J., Jia, J., Shi, L., 2014. A view of iron and steel making technology in the Yan region during the Warring States period and the Han dynasty: scientific study of iron objects excavated from dongheishan site, Hebei province, China. J. Archaeol. Sci. 47, 53–63.

Miller, D., Killick, D., 2004. Slag identification at Southern African archaeological sites. J. Afr. Archaeol. 2, 23–49.

Paynter, S., 2006. Regional variations in bloomery smelting slag of the iron age and roman-british periods. Archaeometry 48, 271–292.

Percy, J., 1864. Metallurgy: the Art of Extracting Metals from Their Ores, and Adapting Them to Various Purposes of Manufacture, vol. 2 Iron; steel. John Murray, London.

Piaskowski, J., 1992. Distinguishing between directly and indirectly smelted iron and steel. Archeomater 6, 169–173.

Rostoker, W., Bronson, B., 1990. Pre-industrial Iron: its Technology and Ethnology. Archeomaterials monographs, Philadelphia, Pa.

Rostoker, W., Dvorak, J., 1990. Wrought irons: distinguishing between processes. Archeomater 4, 153–166.

Shaanxi [Shaanxi Provincial Institute of Archaeology], 2018. Taicheng Ironworks: Report on the Excavation and Research of a Cast Iron Foundry of the Han Period in Yangling, Shaanxi (邰城铸铁:陕西凌汉代铸铁遗址发掘与研究). Shanghai Guji Press, Shanghai (forthcoming).

Shaanxisheng [Shanxi sheng difangzhi bianzuan weiyuanhui], 1993. Shaanxi Provincial Chronograph (Vol. 4): Geology and Minerals Chronograph (陕西省志(第四卷):地质矿产志). Shaanxi Renming press, Xi'an.

Sim, D., 1988. Beyond the Bloom: Bloom Refining and Iron Artifact Production in the Roman World. Publishers of British Archaeological Reports, Oxford.

Török, B., Thiele, A., 2013. Extracting phosphoric iron under laboratory conditions smelting bog iron ores. IOP Conf. Ser. Mater. Sci. Eng. 47, 012034.

Veldhuijzen, H.A., Rehren, T., 2007. Slags and the city: early iron production at Tell Hammeh, Jordan and Tel Beth-Shemesh, Israel. In: La Niece, S., Hook, D., Craddock, P. (Eds.), Metals and Mines: Studies in Archaeometallurgy. Archetype Publications, London, pp. 189–201.

Wagner, D.B., 1993. Iron and Steel in Ancient China. E.J.Brill, Leiden.

Wagner, D.B., 2008. Science and Civilisation in China: vol.5, Chemistry and Chemical Technology, part 11, Ferrous Metallurgy. Cambridge University Press, Cambridge.

Yamada, K., 1998. The development of manual industries and the vicissitudes of government workshops in the Qin and Han dynasties (秦漢代手工業の展開：秦漢代工官の變遷から考える). Toyoshi Kenkyu 56, 701–732 東洋史研究.

Yang, J., Li, Y., Zhao, F., Lou, P., 2014. Experimental studies on the iron objects unearthed from Mapaoquan site in Changping and a discussion of criteria for judging puddling steel (北京昌平马刨泉长城所遗址出土铁器的实验研究———兼论炒钢工艺的一种判据). Chin. J. Hist. Sci. Technol. 35, 177–187 中国科技史杂志.

Zhao, Y., Chong, J., Chen, G., 2012. The Han iron foundry at Taicheng in Yangling, Shaanxi (陕西杨凌邰城汉代铸铁作坊遗址). China Cult. Relics News 2012/3/16 8, 中国文物报.

Zhongguo [Zhongguo yejinshi bianxiezu], 1978. Ancient cast iron technology during the Han period based upon evidence from Guxing (从古荥遗址看汉代生铁冶炼技术). Cult. Relics 2, 44–47 文物.

Zhongguo [Zhongguo shehui kexueyuan kaogu yanjiusuo], 1995. Excavation of an iron foundry site at Han Chang'an city, 1992 (1992年汉长安冶铸遗址发掘简报). Archaeol. 9, 792–798 考古.

Zhongguo [Zhongguo shehui kexueyuan kaogu yanjiusuo], 1997. Excavation of an iron foundry site at Han Chang'an City,1996 (1996年汉长安冶铸遗址发掘简报). Archaeol. 7, 5–12 考古.